# Integrable systems arising from separation of variables on $S^3$

**Diana M.H Nguyen** with *Holger Dullin* · April 2, 2018

THE UNIVERSITY OF SYDNEY

## Geodesic Flow on $S^3$

Consider the sphere $S^3$ as embedded in $\mathbb{R}^4$ with Cartesian coordinates $\boldsymbol{Q} = (x_1, x_2, x_3, x_4)$ and momenta $\boldsymbol{P} = (y_1, y_2, y_3, y_3)$. We obtain a Dirac structure on $T^*S^3$ using the constraints $\boldsymbol{Q} \cdot \boldsymbol{Q} = x_1^2 + x_2^2 + x_3^2 + x_4^2 = 1$ and $\boldsymbol{Q} \cdot \boldsymbol{P} = x_1y_1 + x_2y_2 + x_3y_3 + x_4y_4 = 0$. The geodesic Hamiltonian on this phase space is given by $H = \boldsymbol{P} \cdot \boldsymbol{P} = y_1^2 + y_2^2 + y_3^2 + y_4^2$. This system is known to be superintegrable with a global Hamiltonian $S^1$-action. Taking the quotient of $T^*S^3$ by this action gives the symplectic manifold $S^2 \times S^2$. We perform this reduction by using invariants.

The six angular momenta $\ell_{ij} = x_iy_j - x_jy_i$ form a closed set of invariants and the Hamiltonian can be written in terms of them as $H = \frac{1}{2}\sum_{j>i} \ell_{ij}^2$. Their Poisson algebra has 2 Casimirs: $\mathcal{C}_1 = 2H = \sum_{j>i} \ell_{ij}^2$ and $\mathcal{C}_2 = \ell_{12}\ell_{34} - \ell_{13}\ell_{24} + \ell_{14}\ell_{23} = 0$. The first Casimir is the energy which we fix to 1 and the second is the Plücker relation which is identically 0. Using the $\ell_{ij}$'s as new coordinates we obtain an explicit description of $S^2 \times S^2$ as

$$\mathscr{C}_1 = \mathcal{C}_1 + 2\mathcal{C}_2 = (\ell_{12} + \ell_{34})^2 + (\ell_{13} - \ell_{24})^2 + (\ell_{14} + \ell_{23})^2 = 1$$
$$\mathscr{C}_2 = \mathcal{C}_1 + 2\mathcal{C}_2 = (\ell_{12} - \ell_{34})^2 + (\ell_{13} + \ell_{24})^2 + (\ell_{14} - \ell_{23})^2 = 1.$$

Making the coordinate transformation $(X_1, X_2, X_3) = (\ell_{12} + \ell_{34}, \ell_{13} - \ell_{24}, \ell_{14} + \ell_{23})$ and $(Y_1, Y_2, Y_3) = (\ell_{12} - \ell_{34}, \ell_{13} + \ell_{24}, \ell_{14} - \ell_{23})$ yields a Poison matrix that is block-diagonal and the Poisson algebra is isomorphic to $\mathfrak{so}(3) \times \mathfrak{so}(3)$. It is interesting to note that the $X_i$'s and $Y_i$'s generate the left and right isoclinic rotations in $SO(4)$ respectively. The subgroups of left and right isoclinic rotations are each isomorphic to $SO(3)$, and they give a decomposition of $SO(4)$ as $SO(4)/\{\pm I\} \cong SO(3)_L \times SO(3)_R$.

## Separable coordinates on $S^3$

The Hamiltonian-Jacobi equation of the geodesic flow on $S^3$ separates in the general spherical-elliptical coordinates as well as the 5 degenerate coordinates: prolate, oblate, Lamé-subgroup reduction, spherical and cylindrical coordinates. Schöbel gave an algebraic geometric classification of these coordinates using the Stasheff polytope (Figure 1).

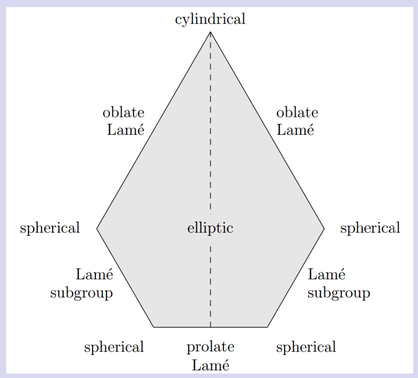


Figure 1: Stasheff polytope for $S^3$ taken from [1]

The 5 degenerate coordinates can be described by appropriate limits of the general elliptical coordinates. Each of these 6 orthogonal coordinate systems gives rise to a Stäckel integrable system on $S^3$. Since the first integrals (given by second-order Killing tensors) are quadratic functions of the angular momenta $\ell_{ij}$, each Stäckel system on $S^3$ descends to an integrable system on $S^2 \times S^2$. In this poster, we attempt to classify these systems by studying features of their integral and action maps.

## The general elliptical coordinates

The general spherical-elliptical coordinates on $S^3$, denoted $(s_1, s_2, s_3)$, are defined as the roots of $K(s) = \sum_{i=1}^4 \frac{x_i^2}{s - e_i} = 0$ where $e_1 \le s_1 \le e_2 \le s_2 \le e_3 \le s_3 \le e_4$. The geodesic Hamiltonian in these coordinate is

$$H = 2\sum_{i=1}^{3} \frac{\prod_{j=1}^4 (s_i - e_j)}{\prod_{k \neq i} (s_j - s_k)}.$$

This system is Liouville integrable with the global polynomial integrals $F_i$ given by

$$F_i = \sum_{j=1, j\neq i}^{4} \frac{(x_iy_j - x_jy_i)^2}{e_i - e_j} = \sum_{j=1, j\neq i}^{4} \frac{\ell_{ij}^2}{e_i - e_j}$$

where $i \in \{1, 2, 3, 4\}$. The $F_i$ satisfy $\sum_{i=1}^4 F_i = 0$ and are related to the separation constants (first integrals) $\eta_1$ and $\eta_2$ by

$$\sum_{i=1}^{4} \frac{F_i}{z - e_i} = \frac{\sum_{i=1}^4 F_i \left(\prod_{j\neq i} (z - e_j)\right)}{\prod_{k=1}^4 (z - e_k)} = \frac{2hz^2 - \eta_1 z + \eta_2}{\prod_{k=1}^4 (z - e_k)} := \frac{R(z)}{A(z)}$$

with $\eta_1 = \sum_{i<j} (e_n + e_m)\, \ell_{ij}^2$ and $\eta_2 = \sum_{i<j} e_n e_m l_{ij}^2$ where the indices $m, n, i, j$ are all distinct. The separated equations are then given by $p_i^2 = -\frac{R(s_i)}{4A(s_i)}$, where $p_i$ is the conjugate momentum to $s_i$. We therefore have three actions:

$$I_i = \frac{1}{2\pi} \int_{r_1}^{r_2} \sqrt{-\frac{R(s_i)}{A(s_i)}}\, ds_i$$

for $i \in \{1, 2, 3\}$, with $r_1$ and $r_2$ being the 2 roots of $R(z)$. Using a Möbius transformation, we show that the sum $I_1 + I_2 + I_3$ is a constant with value equals $\sqrt{2h}$.

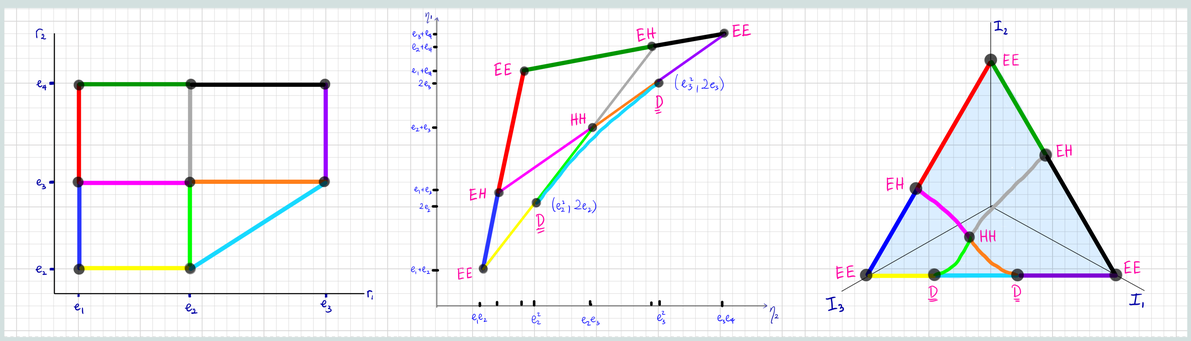

Figure 2: General elliptical coordinate. (a) Roots diagram, (b) Integral map, (c) Action map

## The general elliptical coordinates (cont.)

Figure 2 shows the roots diagram, the integral map and the action map. The integral map consists of 4 lines $\mathscr{L}_i$ with equations $\eta_2 = e_i(\eta_1 - e_i)$ for $i \in \{1, 2, 3, 4\}$ and the quadratic curve $4\eta_2 = \eta_1^2$ which intersects $\mathscr{L}_2$ and $\mathscr{L}_3$ tangentially at the points $(e_2^2, 2e_2)$ and $(e_3^2, 2e_3)$ respectively. This integral map share resounding similarities to that of the geodesics on an ellipsoid and the Neumann problem.

The corresponding action map in Figure 2(c) features the equilateral triangle resulting from the intersection of the plane $I_1 + I_2 + I_3 = 1$ and the positive quadrant. The projection of the image of the action map onto any of the coordinate planes is a Delzant polytope, the inside of which carries additional information in the form of graphs corresponding to the hyperbolic singularities.

## Prolate Lamé Coordinate

The prolate Lamé coordinates are best understood as a degeneration of the general elliptical coordinates with $e_2 = e_3$. In this case, the angular momenta $\ell_{23}$ (or $\ell_{24}$) generates a global $S^1$ action and we have a choice for the integral map (to use either $\ell_{23}$ or $\ell_{23}^2$). Figure 3(b) shows the integral map using $\ell_{23}^2$ and Figure 3(c) uses $\ell_{23}$ (momentum map). This system is known to be a semi-toric system with the existence of a focus-focus type singularity.

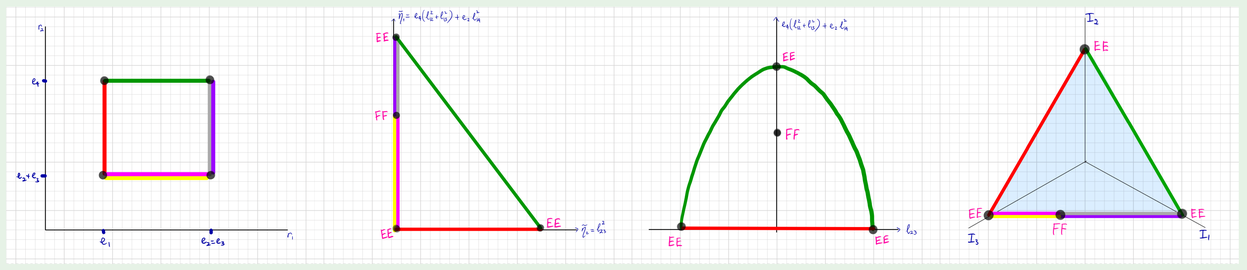

Figure 3: Prolate Lamé Coordinates. (a) Roots diagram, (b) Integral map, (c) Momentum map, (d) Action map

## Oblate Lamé and Cylindrical Coordinates

The oblate Lamé coordinates are degenerations of the elliptical coordinates by setting either $e_1 = e_2$ or $e_3 = e_4$. Again, in this case, we have a global action generated by one of the angular momenta, and so we can "extract the square root" of the integral map to get the momentum map shown in Figure 4.

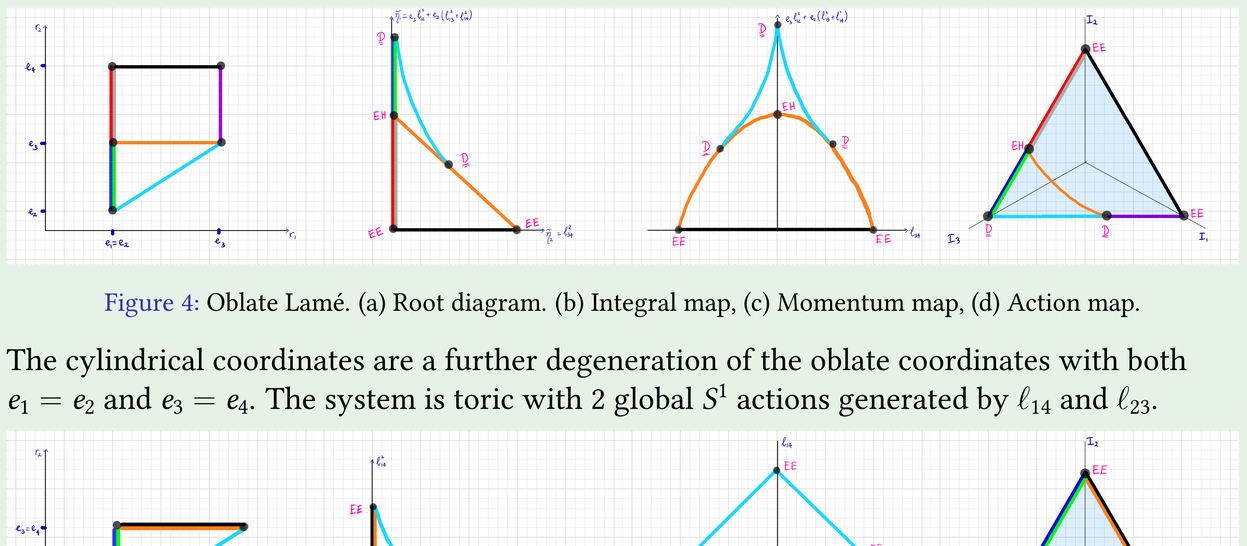

Figure 4: Oblate Lamé. (a) Root diagram. (b) Integral map, (c) Momentum map, (d) Action map.

The cylindrical coordinates are a further degeneration of the oblate coordinates with both $e_1 = e_2$ and $e_3 = e_4$. The system is toric with 2 global $S^1$ actions generated by $\ell_{14}$ and $\ell_{23}$.

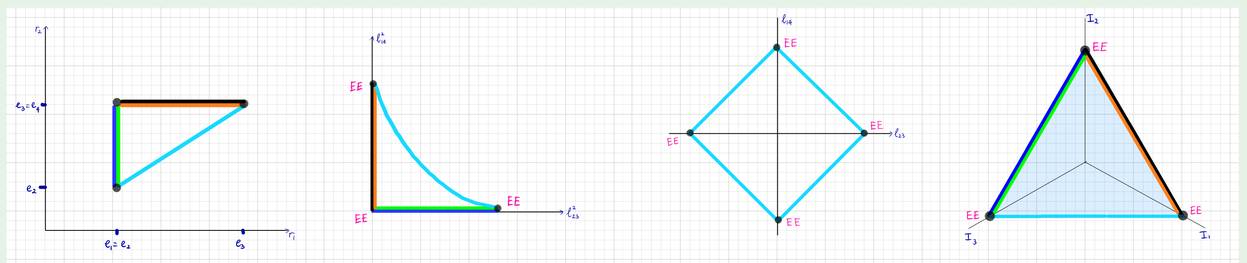

Figure 5: Cylindrical coordinates. (a) Roots diagram, (b) Integral map, (c) Momentum map, (d) Action map

## Lamé reduction and Spherical Coordinates

Lamé reduction and spherical coordinates are extensions of coordinates on $S^2$ onto $S^3$. This is essentially equivalent to setting 3 of the semi-major axes $e_i$ to be equal. Unfortunately, this results in a degenerate root diagram and we no longer have a straightforward correspondence between the roots and the integrals and actions. However, by viewing this as the limit of $e_4 \to \infty$ while keeping $e_1, e_2, e_3$ relatively small, we produce the diagrams in Figure 6(a) and 6(b) for Lamé-reduction and Figure 6(c), 6(d) and 6(e) for spherical coordinates.

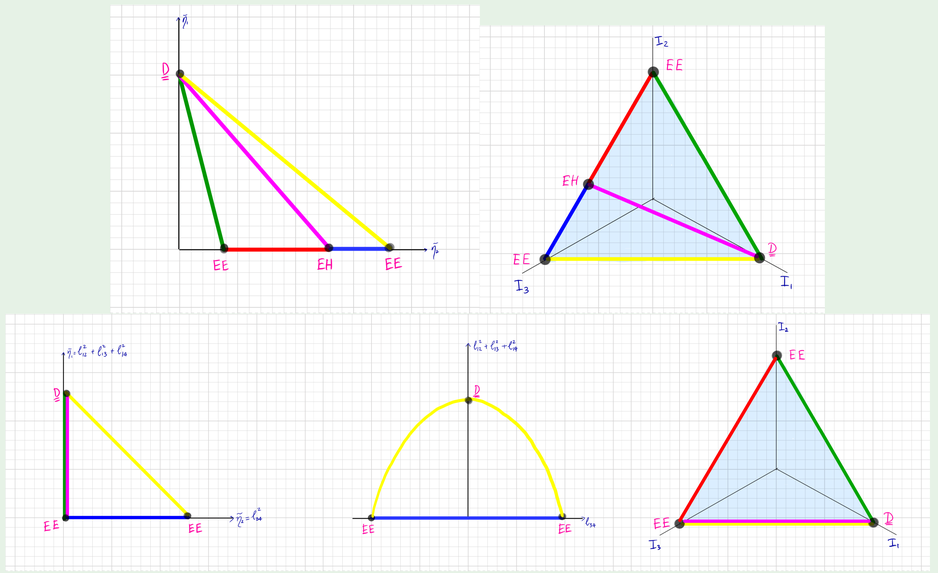

Figure 6: Lamé and Spherical Coordinates. (a) Lamé integral map, (b) Lamé action map, (c) Spherical integral map, (d) Spherical momentum map, (e) Spherical action map

## References

Schöbel, K. (2016). Are Orthogonal Separable Coordinates Really Classified? *Symmetry, Integrability and Geometry: Methods and Applications*. doi:10.3842/sigma.2016.041